ISSN: 2093-5374 / E-ISSN: 2093-5382

R-GAN-NET: A Novel Deep Convolution Neural Network with Augmentation to Detect Lounge Nodules

Asiya[1*], and N. Sugitha[2]

[1*]Research Scholar, CSE Department, Noorul Islam Centre for Higher Education, Tamil Nadu, India. syedasiya14@gmail.com, https://orcid.org/0009-0008-5128-5073

[2]ECE Department, Saveetha Engineering College, Thandalam, Chennai, Tamil Nadu, India. sugithan@saveetha.ac.in, https://orcid.org/0000-0003-0288-333X

Received: November 12, 2024; Revised: December 20, 2024; Accepted: February 13, 2025; Published: March 31, 2025

Abstract

The early identification of lung nodules is important for predicting the development of lung cancer. Lung nodules have a high prospect of turning cancerous, and spotting malignant nodules early improves a patient's recovery prospects. Diagnostic methods currently rely on manual assessment and machine learning, particularly neural network techniques that consider nodule size and color. However, these methods may not be very influential in detecting cancer in its early stages, often taking months or even years to confirm malignancy. Detecting malignant nodules early can significantly extend a person's life. To address this challenge, An R-GAN-NET model proposed an innovative approach that utilizes a R-GAN and deep neural network models to determine whether lung nodules are malignant. For this LIDC-IDRI Kaggle data set is used to train the model. The method effectively deals with small and overlapping nodules by incorporating a Deep Convolutional Network to analyze images and carefully recognize distinct patterns in nodules. The proposed model identifies the malignant nodules without concern for the size or color of the samples. And achieved exceptional performance compared to the prescribed standards, with an accurateness of 96.1%.

Keywords: Deep Learning, CNN, R-GAN, VGG16, LIDC-ID

1 Introduction

Lung cancer is a serious health issue across globe, and early cancer detection and treatment will improve patient life. Lung nodules are growths in small lung tissue, the benign or malignant lung cancer stage. In recent years, several researchers have developed computer-aided detection (CAD) systems and deep learning techniques for automated lung nodule detection, especially in computed tomography (CT) scans (Amaral et al., 2012; Amaral et al., 2013; Sathish Kumar, 2024). CAD systems are introduced to understand the radiologists in identifying the potential nodules. Implementing this model helped improve patient outcomes in diagnosing lung nodules and other medical conditions. However, finally, doctors need to explore the necessary diagnosis and treatment decisions (Bhuvaneswari et al., 2014).

In recent research, Image processing and machine learning techniques have been implemented in the detection and identify lung nodules (Prasad et al., 2011; Koth et al., 2011) The major input to these models are the images of CT, X-Ray and other bio images of lungs. These methods often involved the

Journal of Wireless Mobile Networks, Ubiquitous Computing, and Dependable Applications (JoWUA), volume: 16, number: 1 (March), pp. 488-507. DOI: *10.58346/JOWUA.2025.I1.029*

*Corresponding author: Research Scholar, CSE Department, Noorul Islam Centre for Higher Education, Tamil Nadu, India.

noise reduction in the images, segmentation, feature extraction from the images, and classification with suitable algorithm. In this area Standard techniques are included with rule-based algorithms, region growing, and template matching. They have significantly improved nodule detection rates and become integral to lung cancer screening programs (Sarwar & Sharma, 2014; Nguyen et al., 2023; Sathish & Ravichandran, 2018). Machine learning and neural network standards, like Random Forest, SVM, CNN, VGG16, and others, have been increasingly utilized in recent years for classifying lung nodules. For the initiation of such research, these models require a suitable dataset as input (Chamberlain et al., 2016; Radhika et al., 2019). The machine learning modes need suitable datasets to research nodule classification in this process. Several publicly available datasets are widely used for lung nodule disclosure in medical imaging, particularly chest CT scans (Jyothi & Mary Gladence, 2024). Notable datasets include LIDC-IDRI, a comprehensive resource with thousands of annotated cases, LUNA16, a subset of LIDC-IDRI designed for a challenge, ANODE09, providing diverse nodule types and sizes, NCI's Lung Image Database, Mos Med Data Chest CT Dataset, NIH Chest X-ray Dataset (for X-ray-based nodule detection), and the JSRT and Shenzhen Hospital datasets containing chest X-ray images with nodule annotations (Agarwal et al., 2022; Alshmrani et al., 2023; Kaplan et al., 2021). Researchers and practitioners can leverage these datasets to train and evaluate machine learning and deep learning models for lung nodule detection and classification (Adeshina et al., 2024; Dhurgadevi et al., 2022). However, they should be mindful of data usage policies and ethical considerations when working with medical imaging data (Kazeminia et al., 2020). Machine learning techniques have gained prominence as powerful tools for automating the detection of lung nodules. Traditional techniques often relied on handcrafted features and rule-based systems, which struggled with the diversity and subtleties of nodules in medical images. On the other hand, machine learning algorithms can extract complex patterns and associations from large datasets, improving the precision and reliability of detection (Kavitha, 2024).

Finding lung nodules in medical images involves the application of various neural networks and machine learning models (Puri & Lakhwani, 2013). CNN are a fundamental choice, with architectures like AlexNet, VGG, Inception, and ResNet being commonly used (Kazeminia et al., 2020; Paraschiv & Rotaru, 2020). These models are adept at learning features from CT scans to identify potential nodules. To account for the three-dimensional nature of lung scans, 3D CNNs can be employed, capturing spatial information more effectively. Region-based CNNs (R-CNNs) and variants like Faster R-CNN can pinpoint regions of interest within scans and classify them as nodules or non-nodules (Sharifi et al., 2020; Biradar & Pareek, 2022). U-Net, a popular semantic segmentation architecture, is employed for lung nodule segmentation, outlining nodule boundaries. RNN, especially LSTMs, can process scans slice by slice, maintaining temporal context (Bhattacharjee et al., 2022; Asiya & Sugitha, 2023). Ensemble models combining various architectures can enhance overall detection accuracy. Augmenting the dataset with transformations aids in generalization, and post-processing techniques refine results. Attention mechanisms like Transformers highlight relevant regions, and Explainable AI techniques offer interpretability. Developing a comprehensive lung nodule detection system (Hekmat et al., 2025; Dai et al., 2024). also entails preprocessing for image normalization and noise reduction, rigorous evaluation using clinical metrics, collaboration with medical experts, and adherence to ethical and regulatory standards. This analysis intended to explore and contribute to the growing landscape of lung nodule detection. By leveraging state-of-the-art technologies and methodologies, system can improve the accuracy, efficiency, and clinical utility of early lung nodule identification. This research addresses the technical intricacies of nodule detection and also underscores its profound implications for public health by potentially improving the prognosis of individuals at risk of developing lung cancer.

To address the above challenges, a R-GAN-NET model is implemented, to augment the number samples class wise and balance the dataset, and trained optimized CNN model to capture complex features and classify the results.

1) Contributions

- A novel R-GAN model is implemented to augment the long nodule samples. With predefined threshold values, such as 0.01, to generate additional samples. This approach allowed us to expand our dataset and enhance the representation of long nodule instances.
- Later, a well-optimized CNN model is trained using the augmented dataset. This strategic use of augmented samples contributed to improved model performance, demonstrating the effectiveness of our data augmentation technique.
- To assess the proposed approach's impact, compared the R-GAN-NET model performance, with other prescribed models. The study revealed that the R-GAN-NET model consistently produced robust and superior results compared to alternative models. This underscores the effectiveness of augmentation strategy and the optimized CNN architecture in addressing the dataset's specific challenges.

The article is scheduled as followed: Section 2 concerns the literature review, followed by Section 3, which covers the chosen dataset and describes the augmentation and implementation processes detailed in Section 4. Lastly, Section 5 presents an analysis of the results.

2 Literature Review

Amaral et al., (2012) investigated a clinical decision support system that employs ML algorithms to diagnose pulmonary disease. To determine the most effective classifier, different classification algorithms, including Linear Bayes Normal Classifier, K-Nearest Neighbor, decision trees, ANN, and Support Vector Machine were compared. Features are extracted by using filters, wrappers, and embedded methods. The dataset consisted of 150 measurements from 50 volunteers that contained 25 pulmonary disease and 25 healthy samples. KNN, SVM, and ANN demonstrated the highest suitability among the classifiers examined, yielding highly accurate clinical diagnosis results. (Sathish Kumar, 2024) aimed to enhance the accuracy of early detection of respiratory abnormalities in a cohort of 56 participants, including 28 healthy individuals and 28 smokers with low tobacco consumption, by developing an automated classifier. In this model, the researchers have implemented the KNN and SVM. The KNN achieved an accurateness of 0.89, and SVM an accuracy of 0.87.

O’Neil et al., (2017) compared two different approaches to classify pulmonary nodules on CT scans using an AI-based solution. The first approach focused on "manmade" features, which were derived from traditional handcrafted texture descriptors. The second approach centered around "machine-made" features and utilized deep learning CNNs. The study utilized a dataset consisting of high-resolution ILD CT images and included five different tissue patterns. This model got results using CNN-based approach secured a higher accurateness of 69.9%, compared to the handcrafted method which attained an accuracy of 65.5%. (Altan et al., 2019). conducted research to analyze COPD by employing deep learning techniques. Several machine learning algorithms were utilized to recognize COPD early on by analyzing multi-channel lung sounds. The study primarily aimed to research these lung sounds by extracting statistical features related to frequency modulations obtained through the Hilbert-Huang transform. As a result of this research, the standard secured accurateness of 93.67%, sensitivity of 91%, and specificity

of 96.33%. (Mkindu et al., 2023) analyzed the use of deep learning to inspect respiratory sounds. This study researched a 3D spatial framework that incorporated three data points within the signal. The focus of this paper was on categorization of lung sounds at-risk levels and advanced stages of COPD. The researcher used a dataset named Respiratory Database@TR for lung sounds and chose the Deep Belief Networks algorithm for classification. In this paper, feature extraction was done using 3D-SODP. The resulting model got precision, sensitivity, and specificity rates of 95.84%, 93.34%, and 93.65%, correspondingly.

Boban & Megalingam, (2020) conducted research on lung disease, analyzing 400 CT scan images of various conditions. To examine the scan images, they used three classifiers: KNN, SVM, and MLP (Alzaidi, 2024). The GLCM was used as a feature extraction method. The results indicated that MLP had an accuracy rate of 98%, while SVM achieved 70.45% and KNN received 99.2%. Trusculescu et al., (2020) have focused at promptly detecting idiopathic pulmonary fibrosis (IPF) disease. This study utilized a natural dataset and the AlexNet convolutional neural network model. The author integrated ReLU layers for effective feature extraction and got an accuracy of 70.7%.

Wang et al., (2020) have examined AECOPDs by analyzing a dataset of electronic medical records (EMRs) from 2011 to 2017. The focus was on patients with COPD. The researchers used various ML algorithms to analyze the data, including Support Vector Machine, Logistic Regression, random forest, Naïve Bayes and KNN. They also utilized label or one-hot encoding methods for extracting features. The results got a sensitivity of 0.75 using k-means clustering and 0.80 using the support vector machine approach. (Biradar & Pareek, 2022) introduced a 2D-CNN algorithm for organizing malignant and non-malignant lung cells in CT scans. Utilizing a Kaggle dataset, the standard reached an accurateness of 88.76% in differentiating between cancerous and non-cancerous lung nodules. This approach is touted as more efficient than conventional neural networks for this task, potentially implying advantages in computational efficiency or model performance.

(Saikia et al., 2022) concentrated on classifying lung nodules into four types using CT scan images (small-cell carcinoma, adenocarcinoma, squamous-cell carcinoma, and large-cell carcinoma). It proposes a hybrid algorithm, combining VGG networks with SVM and random forests, effectively reducing computational complexity and achieving an impressive 98.70% accuracy in classification. Bhattacharjee et al. (Bhattacharjee et al., 2022) have introduced an innovative approach, a hybrid system was devised, combining an optimized Random Forest classifier with a K-means visualization tool, to address the classification of malignant and non-malignant cases in medical imaging data. Through rigorous hyper parameter optimization, the Random Forest model was finely tuned to yield optimal results. Meanwhile, K-means clustering was employed for insightful data visualization, facilitating the identification of distinct malignant and non-malignant clusters. Impressively, the finest model, after undergoing four rounds of hyper parameter optimization, achieved a remarkable 10-fold cross-validation exactness rate of 92.14% when applied to the challenging LIDC-IDRI dataset.

Rehman et al., (2021) have introduced an innovative lung cancer detection and classification technique using machine learning. This system involves feature extraction and fusion, combining patch-based LBP and DCT on chest CT scan images and classification using SVM and KNN. The dataset evaluation demonstrates impressive performance with 93% precision for Support Vector Machine and 91% for K-Nearest Neighbor. (Jian et al., 2023) introduced 3DAGNet, an advanced 3D CNN designed for the intelligent classification and diagnosis of lung nodules in CT scans. It incorporated a spatial attention and search module motivated by the diagnostic process of physicians, allowing it to focus on relevant regions and capture context across the entire volume. The model also features a multi-scale cascade module that enhances detection through attention, search, and contextual feature fusion. In

experimental tests on the LUNA16 dataset, the 3DAGNet achieved an impressive sensitivity of 88.08% on the average FROC score, demonstrating its efficiency in accurately identifying lung nodules, a critical task in medical image analysis.

(Shahzad et al., 2024) have introduced a novel 3D framework, IR-UNet++, for automated pulmonary nodule disclosure. Combining components from Inception Net and ResNet, it enhances feature extraction with a squeeze-and-excitation structure and incorporates short skip pathways in a U-shaped network design. Experimental evaluations on the LUNA16 dataset demonstrate its superior performance compared to existing methods, with sensitivity rates of 90.13%, 94.77%, and 95.78% at false positive rates of 1 FP/scan, 4 FPs/scan, and 8 FPs/scan, respectively. These results indicate the effectiveness of IR-UNet++ in improving lung nodule detection, holding significant promise for early diagnosis and treatment of pulmonary diseases. (Kovalev & Kazlouski, 2019) have investigated image processing to improve the number of samples by using GAN. They researched the bio-medical image classification to classify the various scanned images of the human body. They experimented on the realistic chest X-Ray images and implemented the Random forest standard to classify the data. They achieved 82% accuracy after augmenting the dataset by using GAN.

Limitations of Related work: Many of the systems worked on lung nodule identification, with and without augmentation with simple or complex models and provided good accuracy. But most of the systems augmented samples statistically like rotation, adding manual noise, rotating images certain angles etc. to increase the number of samples.

3 Dataset

In this research, a LIDC-IDRI dataset and Lung image set from kaggle used that contains the total 1018 cases and each which contains the CT images and that are collected from the 1010 patients (www.kaggle.com). These images are classified into three groups of classes that are: nodules smaller than 3mm, nodules larger than 3mm, and non-nodule samples. All annotations, along with the number of nodules in each image, are stored in XML files. This dataset plays a key role in the improvement of computer-aided diagnosis systems and deep learning models for the early detection of malignant lung nodules, offering a consensus view from multiple radiologists to enhance the robustness of algorithms. The provided annotations and the number of nodules present in each sample are given d in an XML file. Table 1 illustrates the count of data samples in class from LIDC-IDRI.

Table 1: Nodule Count for Each Sample, Total Number of Samples from LIDC-IDRI

Total Number of samples with 0 nodules found on CT image	Total number of nodules with nodule size <=3mm	Total number of nodules with nodule size >=3mm	Total samples
20	877	857	1012(before augmentation)
3000	3000	3000	9000(after augmentation)

From Table 1, out of the 1012 samples, it is observed that only 20 samples do not contain any nodules. The remaining 992 samples exhibit nodules of various sizes, including those smaller than or equal to 3 mm and those larger than 3mm. additionally, some of the images have both sizes of nodules together. Figure 1 and 2 illustrates the samples images of lung nodules from both datasets.

1) Data Augmentation with R-GAN

To progress the accuracy of our machine learning system for image processing, it is requiring a sufficient number of data samples for training and testing. And the data set consist very less number of samples and imbalance samples. Therefore, R-GAN is applied data augmentation techniques to enrich our dataset. Through this process, the augmentation process applies various transformations and adjustments to the images, creating new samples and increasing the data points. The primary goal of data augmentation is to enhance the model's performance and accuracy by increasing the number of data samples. Popular augmentation methods include rotation, blur, brightness adjustment, and scaling.

In this an R-GAN algorithm implemented to generate artificial images. R-GAN is a type of Generative Adversarial Network that incorporates regularization techniques into the training process. One approach used here involves intentionally fixing the loss function to a certain threshold, such as (N_{sp}), which introduces a controlled amount of noise to the generated images. The model learns to recognize and handle adversarial images by including such noised data.

The augmented dataset exposes the model to a wider range of challenging examples by utilizing R-GAN with fixed loss thresholds and generating artificially noised images. This helps the model become more robust and adept at handling diverse and potentially adversarial scenarios, ultimately enhancing its performance and generalization capabilities in computer vision and deep learning tasks.

Loss of Discriminator is $L_D = \text{Error}(D(x), 1) + \text{Error}(D(G(x), 0))$ and loss function for Generator is $L_G = \text{Error}(D(G(x)), 1)$ from this with cross entropy loss function. The author optimized the both the losses with respect toN_{sp}. From equation (1) a threshold noise is added like N_{sp} and it is further simplified to equation (2) and (3). The loss between generator and discriminator is found with equation (4) that if further simplified to equation (5).

$$\frac{p_{data}(x)}{D(x)} = N_{sp} + \frac{p_g(x)}{1-D(x)} \quad (1)$$

$$\frac{p_{data}(x)}{D(x)} = \frac{N_{sp} - N_{sp}D(x) + p_g(x)}{1-D(x)} \quad (2)$$

$$D(x) = \frac{(1-D(x))p_{data}(x)}{N_{sp} - N_{sp}D(x) + p_g(x)} \quad (3)$$

$$V(G,D) = E_{x-p_{data}}[log\ (D(x)] + E_{x-p_g}[log\ (1-D(x)] \quad (4)$$

$$V(G,D) = E_{x-p_{data}}\left[log\left(\frac{(1-D(x)p_{data}(x)}{N_{sp}-N_{sp}D(x)+p_g(x)}\right)\right] + E_{x-p_g}\left[log\left(1-\frac{1-D(x)p_{data}(x)}{N_{sp}-N_{sp}D(x)+p_g(x)}\right)\right] \quad (5)$$

Where N_{sp} is the noised data, range between $0<N_{sp} \leq 1$. Equation (5) is the derived optimizer for R-GAN. And x is the real data, G(x) synthetic data, D(x) discriminator evaluation for real data, and D (G(x)) is generator evaluation for synthetic data, Figure 1 shows the various nodule sizes of CT scan images. Figure 3 illustrates the working structure of R-GAN. Table 2 presented the R-GAN –NET algorithm.

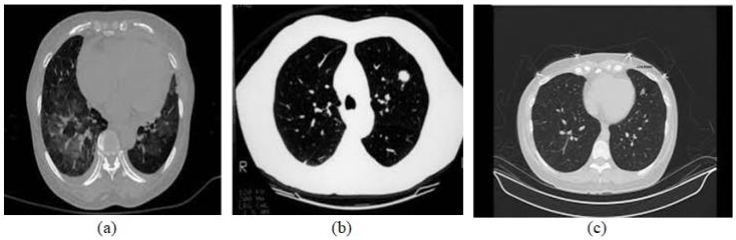

Figure 1: (a) CT-image with<3mm Lung Nodules (b) CT-image >3mm Lung Nodules (c) CT-image with Artificial Lung Nodules

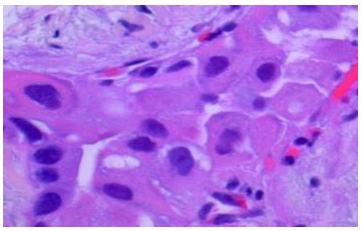

Figure 2: Lung Nodule Image Sample

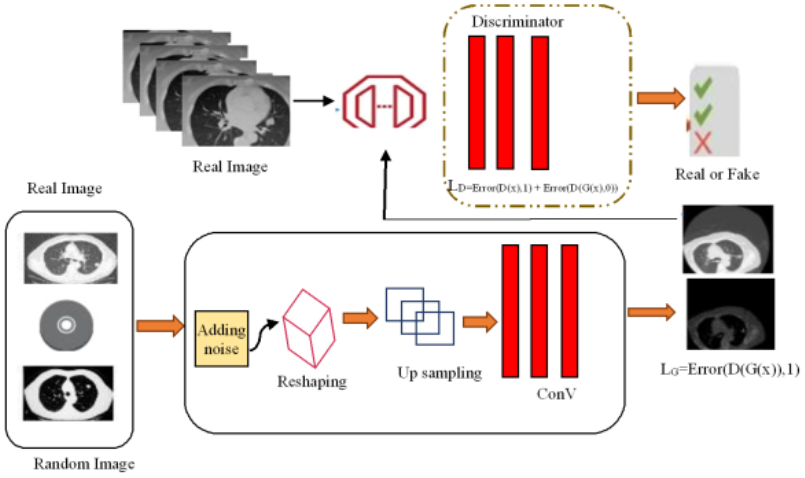

Figure 3: Working Structure of Regularized GAN

Table 2: Algorithm for R-GAN-NET

Algorithm : R − GAN-NET
R-GAN (real_data, Noise, loss): *Rd=real_data;* *N=Noise* *L=loss* *N_image=Generator (Rd,n,l);* *return N_image* *Generator(R,N,l):* *Im=probability_randome_image (R, N)* *Min=loss (Error (D (Im), 1)* *R=Discriminator (Im,Rd)* *return Im* *Discriminator (Im,Rd):* *Loss=Max (Error (Rd, 1) +error (Im, 0)* *Generator (loss,Rd,Im)* *return loss* *O-CNN(N_image(x),lear_rate,iterations):* *While (i<iterations):* $\sum(i * w)(x, y)$ $p(x, y) = Max\_Pool(f)(x, y)$ $y = f(wx + b)$ $retunloss(y_{true}, y_{pred}) = \frac{1}{m} - \sum_{c=1}^{C}(y_c \log(p_c))$

Following data augmentation, the dataset was meticulously balanced to ensure equitable representation of all classes. These augmented data samples were pivotal in training our R-GAN-NET model. We amassed 9,000 samples, with 3,000 samples belonging to each class.

To establish distinct training, testing, and validation sets, we partitioned these 9,000 samples. Consequently, we allocated 7,200 samples for training, 900 for testing, and retained 900 for validation purposes.

Balancing the dataset and creating these distinct subsets was a strategic approach to empower our model with the ability to learn effectively across all classes, finally improving its performance in classification tasks? Figure 4 represents the original samples of lung nodule. Figure 5 illustrate the generated samples by R-GAN model where the generator loss<=1. Figure 6 presents the R-GAN generated samples where generator loss>2.

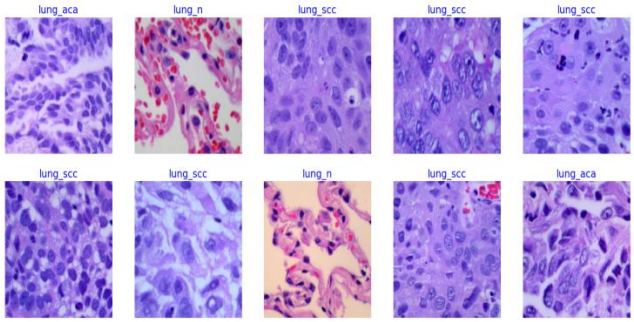

Figure 4: Original Samples of Lung Nodule

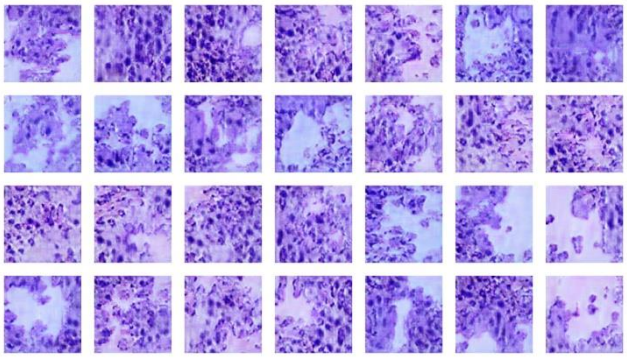

Figure 5: R-GAN Generated Samples where Generator Loss<=1

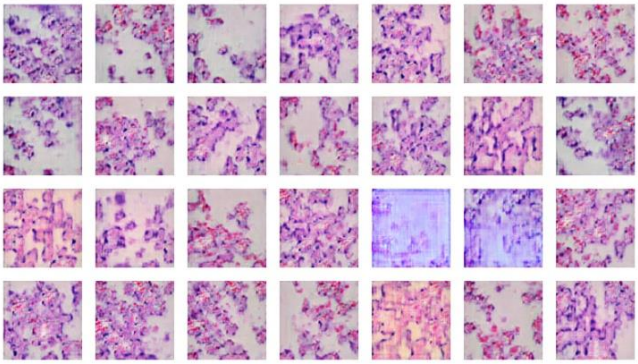

Figure 6: R-GAN Generated Samples where Generator Loss>2

4 Implementation

A sophisticated deep learning model leveraging R-GAN-NET to segment and precisely detect lung nodules within CT scans precisely. Interpreting these images presents a unique challenge, primarily when identifying slight anomalies such as lung nodules. According to previous research, the Deep learning techniques have performed better in image classification and detection processes, conclusively improving the accuracy and effectiveness of diagnostic procedures. Figure 7 shows the architecture for the proposed methodology. Where C1 represents the adenocarcinoma class of dataset, C2 represents squamous cell carcinoma class of dataset and C3 illustrate the small scale lung cancer.

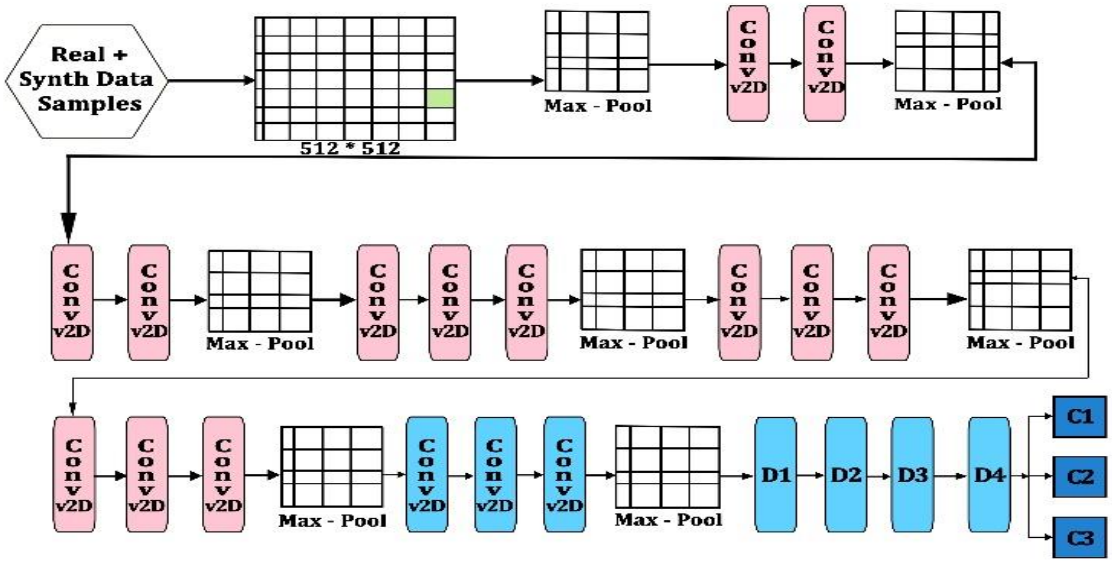

Figure 7: Customized CNN Model Architecture

The developed deep learning model, depicted in Figure 7, was designed to detect small nodules in CT images. After image augmentation with R-GAN and before feeding the images into the system, we applied the preprocessing methods to convert the base image to grayscale. Then, we resized all the images to 512x512 proportions. The model architecture consisted of five convolutional layers with max pooling for nodule identification, followed by four fully connected dense layers and final layer utilized a softmax activation function.

The core architecture consists of five convolutional layers, max-pooling operations for feature extraction, and four fully connected dense layers for further processing. The final output layer uses softmax activation with three dimensions, indicating a classification task with three possible classes. A mathematical convolution operation extracts features within the convolutional layers by applying learned filters to the input image, resulting in feature maps. The final layer utilized a softmax activation function with dimensions of 3x1 for output.

The process of extracting features from the input image (I) involves the use of convolutional layers to perform convolution operations using learned filters (W). The result of this process contains the set of feature maps (F). Along with the result also included with the convolution operation that presented in the equation (6), that involves multiplying each element of the filter (W) with the corresponding element

of the input image (I), then summing the results to obtain a single scalar value at each spatial coordinate (x, y).

$$f(x,y) = \sum(I * W)(x,y) \quad (6)$$

The pooling layers basically implemented for diminished the dimensions of the feature maps through down sampling methods be like max pooling (equation 7). The pooling operation (Pool) takes place at spatial coordinates (x, y) to produce the resulting pooled feature maps.

$$p(x,y) = Max_{Pool(f)(x,y)} \quad (7)$$

$$y = f(wx + b) \quad (8)$$

$$loss(y_{true}, y_{pred}) = \frac{1}{m} - \sum_{c=1}^{C} [\![(y_c]\!] \, log(p_c)) \quad (9)$$

The classification process ends with dense layers, which combine high-level features extracted by convolutional layers, enabling the network to learn difficult patterns and relationships in the data. These layers introduce non-linearity through activation functions and were often utilized for categorization or regression tasks, making them the final layers in Neural Networks. They can also diminish the dimensionality of feature maps when needed. These layers perform the linear transformation on the input data, as depicted in Equation (9). These transformations relied on the adjustable parameters, specifically weights (W) and biases (b).

During the training process, our model was able to match input images with their respective predictions via forward propagation. During the classification stage, the standard's predictions were measured against the real ground truth labels with a specific loss function, like cross-entropy, as described in equation (8). This loss function evaluated the variation between the predicted probabilities (p_c) and the actual labels (y_c) for every class (c).

Here is an overview of the essential hyper parameters used in our model, which you can find in Table 2. We chose a learning rate of 0.001, a typical value to train our R-GAN-NET model. We also included a dropout rate of 0.03 to avoid over fitting. In each training iteration our model designed to drop the 3% of the parameters to prevent the over fitting. The Adam optimizer algorithm implemented in our proposed model to control the learning rate in the NN models.

5 Results and Analysis

The LIDC-IDRI Kaggle dataset is used to train the model for identifies the lung nodules accurately. In this dataset, three types of CT image classes are available: "no nodule," "<3mm nodule size," and ">3mm nodule size." We proposed the R-GAN-NET, a deep learning model, to improve the precision of identifying lung nodules. We trained it for 100 epochs while setting the hyperparameters to optimize the classification results. The proposed system got a remarkable accurateness of 0.961 and effectively distinguished between true positive and false negative values, and that is critical for accurate classification. Furthermore, our model can detect artificial nodules, including those with image interference. We incorporated adversarial augmentation during the image augmentation process to enhance our model's robustness. This involved introducing artificial images with minimal noise N_{sp} into the training data. Training of our model on these negative images allowed us to identify and diagnose artificial nodules effectively. Consequently, we utilized R-GAN to augment the data and generate synthetic images. Instead of exclusively optimizing the loss function to a minimum, we applied regularization techniques to the loss function. This regularization allowed for better control and regularization of the generated images. These processes contribute to the improved outcome of proposed system. Table 3 represents the optimized results of R-GAN-NET. We utilized a dynamic learning rate

to optimize the model, starting with a learning rate 0.001. After five iterations, the rate adjusted to 0.0005; after eight iterations, the learning rate changed to 0.00025. Subsequently, it has changed to 0.00013 for the next iteration. The learning rate decreased gradually with each iteration until it reached 0.00001, at which point the accuracy was 0.961. The model experimented with different batch sizes, including 16, 32, and 64, to determine the most suitable size for the model. Our observation revealed that the 16 batch size was too small and resulted in under fitting, while batch size 64 exhibited bias in accuracy and recall. Finally, we found that a batch size of 32 produced the best-fit standard with optimal precision, recall, and F1 score, as represented in tables 4, 5, and 6, illustrating the accuracy, precision, recall, and F1 score results for all tested batch sizes.

Table 3: R-GAN NET Model Results for Tuned Hyper Parameters

	Precision	Recall	F1-score	Support
0	0.87	0.98	0.93	1000
1	0.91	0.92	0.92	1000
2	0.98	0.86	0.92	1000
Accuracy			0.961	3000
Macro avg	0.95	0.95	0.960	3000
Weighted Avg	0.95	0.95	0.961	3000

Table 4: Accuracy and Precision Score for Different Test Sizes where Batch Size=16(average of 3 Classes)

Batch_size=16	Accuracy	Precision	Recall	F1-Score
Test_size=20	0.87	0.89	0.95	0.91
Test_size=25	0.88	0.89	0.92	0.90
Test_size=30	0.88	0.891	0.92	0.91

Table 5: Accuracy and Precision Score for Different Test Sizes where Batch Size=32(average of 3 Classes)

Batch_size=32	Accuracy	Precision	Recall	F1-Score
Test_size=20	0.92	0.93	0.92	0.91
Test_size=25	0.961	0.95	0.95	0.954
Test_size=30	0.960	0.951	0.95	0.954

Table 6: Accuracy and Precision Score for Different Test Sizes where Batch Size=64(average of 3 Classes)

Batch_size=64	Accuracy	Precision	Recall	F1-Score
Test_size=20	0.87	0.82	0.80	0.82
Test_size=25	0.87	0.81	0.81	0.83
Test_size=30	0.88	0.81	0.81	0.83

The research objective was to increase the efficiency of the standard by reducing the number of parameters used, while ensuring its effectiveness. Figure 9 indicates that the model performed well, with high true positive rates and low false negatives, indicating a strong fit to the data. However, the significance of evaluating the model's capacity to simplify beyond its training dataset, which accomplished through separate validation tests. Figure 8 shows the training and validation loss, revealing a consistent decrease in loss with each epoch, accompanied by an enhancement in the standard’s accuracy during the training procedure.

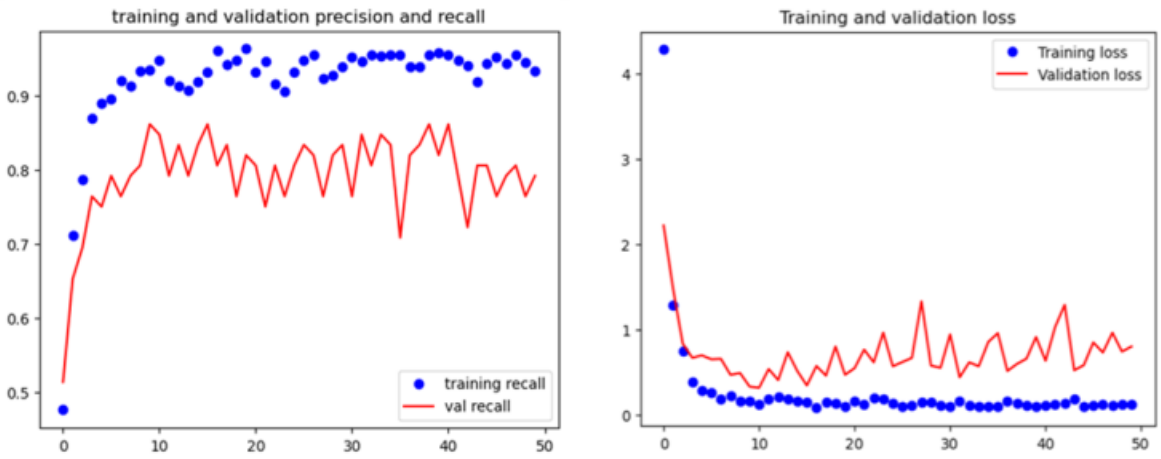

Figure 8: Accuracy and Loss of Proposed R-GAN-CNN Model

Figure 8 illustrates a visual representation of the R-GAN-NET model's training and validation accuracy over 100 epochs. This visualization explains that the sample's performance goes beyond simply remembering the training data. Constant values across various classes represent the standard's stability and neutrality, indicating that it does not indicate bias towards any specific class. The proposed model had performed well than all other prescribed models, including the standard VGG16 and R-GAN-CNN models. The comparison of all specified models and including proposed measures presented in the table 7. In Figure 9, the accuracy among different classes of the dataset of proposed model R-GNN-NET by using confusion matrix. The observations revealed that GAN-NET model performed well. From figure 8 the model is getting little over fitted, in the future will address the issue by providing optimal model.

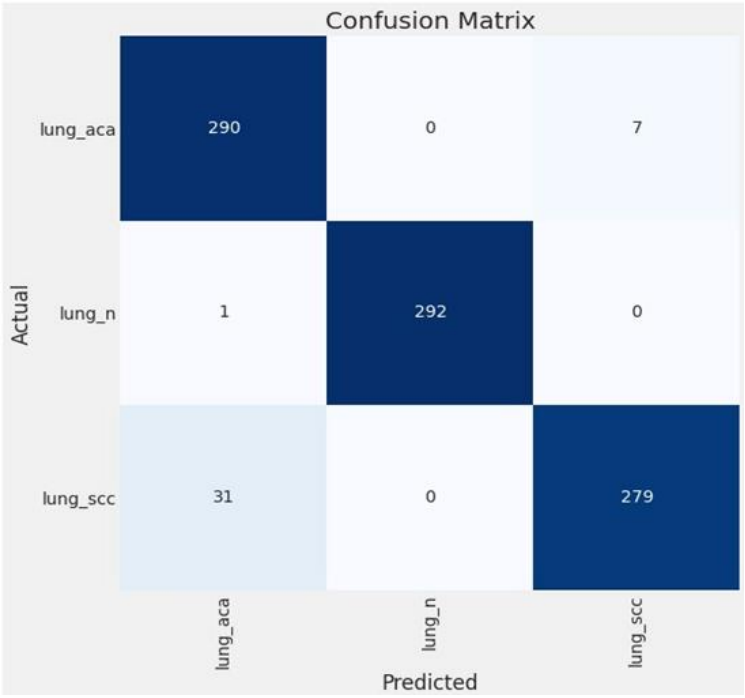

Figure 9: Confusion Matrix of R-GAN_NET

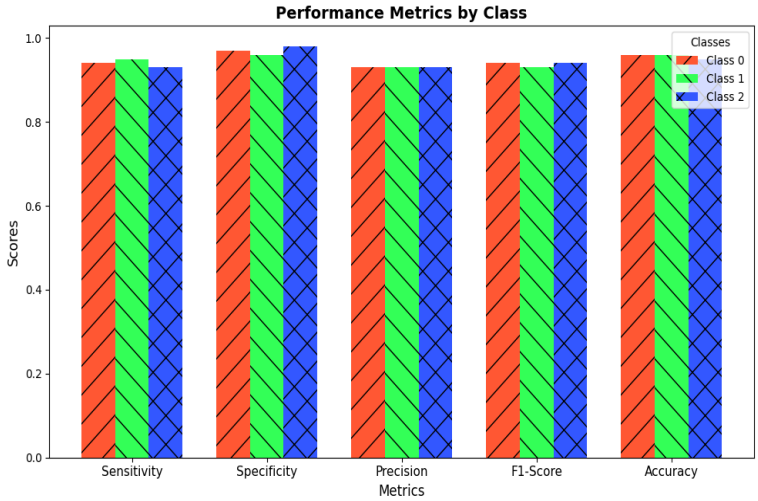

Figure 10: Confusion Matrix of R-GAN_NET

Figure 10 demonstrates that the model performs well across different types of lung nodules. It is highly accurate in identifying positive cases and avoids errors with negative cases, and this stresses the model's diagnostic solid abilities, building it a reliable tool for detecting nodules. These results stay constant and accurate, portraying the mechanism's capacity to address different input data effectively.

The ROC curve from Figure 11 analysis reinforces this, with near-perfect scores for each class, signaling that the prototype can effectively differentiate between different types of lung nodules, and these high scores suggest that the model is unlikely to make incorrect predictions, maintaining a high confidence level in its ability to separate positive from negative cases across all lung nodule types.

Moreover, the precision-recall curves from figure 12 reflect the benchmark's capacity to maintain high correctness in its predictions while covering a broad range of actual cases. The graph showed that the system consistently makes accurate classifications, even as the number of identified instances increases, which is essential in medical diagnostics to ensure that positive cases are captured without overwhelming errors.

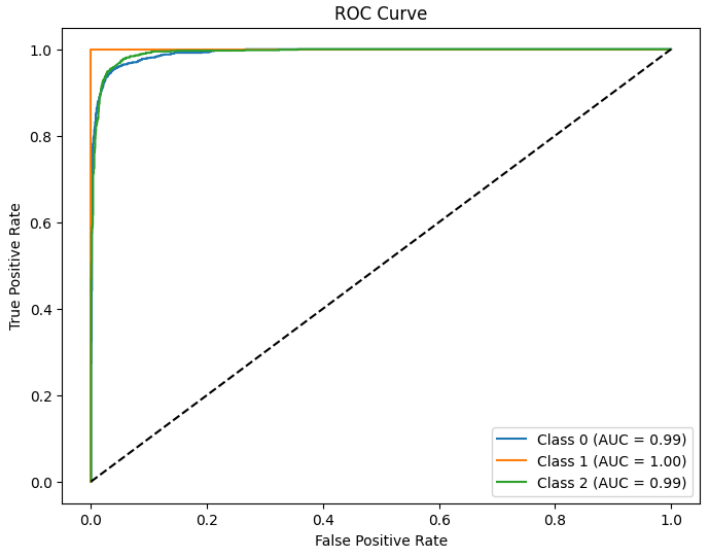

Figure 11: ROC Curve of R-GAN_NET

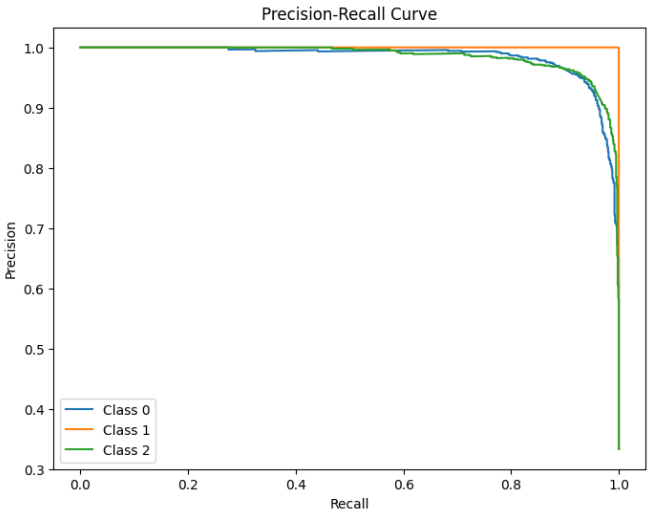

Figure 12: Precision- Recall Curve of R-GAN_NET

TABLE 7: Results Various Models and Proposed Model (R-GAN-NET).

Reference	Dataset	Model	Results	Area
(Amaral et al., 2012)	Med Gift ILD Database	SVM	Accuracy:98.2%	Lung Disease
(Bhuvaneswari et al., 2014)	CT Dataset	Multilayer Perception Neural Networks (MLP-NN)	F1-Score:0.92	Lung Disease
(Bodduluri et al., 2013)		KNN	Accuracy:92%	Pulmonary Disease
(Emanet et al., 2014)	Synthetic	SVM	Accuracy:88%	Pulmonary Disease
(Hosseinzadeh et al., 2013)	Final Cleaned database (FCdb)	SVM	Accuracy:91.2%	Lung Tumor
(Palaniappan et al., 2014)	R.A.L.E	SVM	Accuracy:92.19%	Pulmonary Disease
		KNN	Accuracy:92.10%	
(Kim et al., 2018)	ROI	CNN	Accuracy:95.12%	Interstitial Lung Disease(ILDs)
(Ma et al., 2019)	ICBHI 2017 DATASET	Deep learning - Bi-ResNet (BRN) model	Accuracy:50.16%	Respiratory Disease
(Poreva et al., 2017)	Synthetic dataset	SVM	F1-Score:75%	Lung diseases
		Decision Tree	F1-Score:72%	
(Rehman et al., 2021)	CT scan images dataset	SVM	Accuracy:93%	Lung Cancer
		KNN	Accuracy:91%	
(Jian et al., 2023)	LUNA16 dataset	3DAGNet	Accuracy:88.8%	Pulmonary Nodule Detection
(Lin et al., 2023)	LIDC-IDRI	3D-CNN custom VGG16 model	Accuracy:95%	Lung Nodule Identification
Proposed Models	**LIDC-IDRI**	**R-GAN-NET**	**Accuracy:96.1%**	**Lung nodule identification**
		R-GAN-CNN	**Accuracy:95.4%**	**Lung Nodule Identification**

Table 7 gives a thorough comparison of the performance of different methods from previous studies and the proposed R-GAN-NET model for lung nodule and pulmonary disease detection. Several

traditional models, such as SVM and K.N.N., have demonstrated notable accuracy. For instance, SVM models applied to the MedGift I.L.D. Database and the Final Cleaned Database (FCdb) got 98.2% and 91.2% accuracy rates, correspondingly, highlighting their strong performance in detecting lung disease and tumors. Similarly, K.N.N. models have achieved accuracy levels of up to 92.1% for pulmonary diseases, as seen in results from the R.A.L.E. database.

More complex standards like CNN and 3D networks have also shown good results. For instance, a custom 3D-CNN VGG16 model got 95% accuracy on the LIDC-IDRI dataset for lung nodule identification, demonstrating the increasing capability of deep learning approaches in handling complex medical imaging tasks. The 3DAGNet, used to the LUNA16 dataset for pulmonary nodule identification, gained a precision of 88.8%, further representing the utility of 3D-based approaches.

Models, like the Bi-ResNet (BRN) prototype used for the ICBHI 2017 dataset, worked with more challenging datasets and got only 50.16% exactness. This highlights the current challenges in respiratory disease detection, and therefore, accuracy can differ depending on the dataset and system architecture. In contrast, the proposed R-GAN-NET model outperforms many existing models, achieving 96.1% accuracy on the LIDC-IDRI dataset for lung nodule identification. At the same time, its variant, R-GAN-CNN, reaches 95.4% accuracy. These outcomes explained the superior performance of the R-GAN-NET, and that advanced data augmentation and deep learning techniques to achieve higher accuracy levels than most previous approaches.

6 Conclusion

In this paper R-GAN-NET model is implemented to identify lung cancer based on the presence of lung nodules, focusing on various types of lung cancer, including adenocarcinoma, squamous, and small-scale lung cancer. To overcome the challenge of limited data availability, our model employed Regularized GAN to generate synthetic samples, thereby increasing the size of the dataset. Various hyperparameters, like batch size and dynamic learning rate, were fine-tuned to identify the optimal model configuration. Ultimately, it's found that the optimized R-GAN-NET method secured a remarkable exactness of 0.961. The model was trained over 100 epochs, with a batch size of 32 and a learning rate of 0.00001. An important aspect of this investigation is comparing the proposed R-GAN-NET standard with other established benchmarks, and through this comparative analysis, the presented model consistently topped the alternative models on the test samples, reaffirming its effectiveness in the context of lung cancer prediction. The outcomes demonstrate favorable prospects for using this model in clinical practice to enhance the precision and effectiveness of lung cancer diagnosis.

Future Work: The future work involves of implementing more optimized and robust model, because our proposed model slightly over fitted, that will be overcome. And will work multiple disease detections.

7 Abbreviations

RNN	Recurrent Neural Network
GAN	Generative Adversarial Network
ML	Machine Learning
LBP	Local Binary Pattern
DCT	Discrete Cosine Transform
CNN	Convolutional Neural Networks
CT	Computed Tomography

ANN	Artificial Neural Networks
R-GAN	Regularized- Generative Adversarial Network
SVM	Support Vector Machines
N_{sp}	Net threshold error
D(x)	Discriminated data
G(x)	Generated data
L_D	Discriminated loss
L_G	Generator loss
I	Identity Matrix
W	Weights
y_{true}	Actual lable
y_{pred}	Predicted values
b	Bias
LSTM	Long Short-Term Memory
KNN	K-Nearest Neighbor

Data Availability: The used in this study is available at https://www.kaggle.com/datasets/andrewmvd/lung-and-colon-cancer-histopathological-images

Author Contribution: All author equally contributed.

References

[1] Adeshina, A. M., Anjorin, S. O., & Razak, S. F. A. (2024). Safety in Connected Health Network: Predicting and Detecting Hidden Information in Data Using Multilayer Perception Deep Learning Model. *Journal of Internet Services and Information Security, 14*(4), 524-541. https://doi.org/10.58346/JISIS.2024.I4.033.

[2] Agarwal, V., Lohani, M. C., Bist, A. S., & Julianingsih, D. (2022). Application of voting based approach on deep learning algorithm for lung disease classification. In *2022 International Conference on Science and Technology (ICOSTECH*. 01-07. IEEE. https://doi.org/10.1109/ICOSTECH54296.2022.9828806.

[3] Alshmrani, G. M. M., Ni, Q., Jiang, R., Pervaiz, H., & Elshennawy, N. M. (2023). A deep learning architecture for multi-class lung diseases classification using chest X-ray (CXR) images. *Alexandria Engineering Journal*, *64*, 923-935. https://doi.org/10.1016/j.aej.2022.10.053.

[4] Altan, G., Kutlu, Y., & Allahverdi, N. (2019). Deep learning on computerized analysis of chronic obstructive pulmonary disease. *IEEE journal of biomedical and health informatics*, *24*(5), 1344-1350. https://doi.org/10.1109/JBHI.2019.2931395.

[5] Alzaidi, E. R. (2024). Optimization of Deep Learning Models to Predict Lung Cancer Using Chest X-Ray Images. *International Academic Journal of Science and Engineering*, *11*(1), 351–361. https://doi.org/10.9756/IAJSE/V11I1/IAJSE1140

[6] Amaral, J. L., Lopes, A. J., Jansen, J. M., Faria, A. C., & Melo, P. L. (2012). Machine learning algorithms and forced oscillation measurements applied to the automatic identification of chronic obstructive pulmonary disease. *Computer methods and programs in biomedicine*, *105*(3), 183-193.

[7] Amaral, J. L., Lopes, A. J., Jansen, J. M., Faria, A. C., & Melo, P. L. (2013). An improved method of early diagnosis of smoking-induced respiratory changes using machine learning algorithms. *Computer methods and programs in biomedicine*, *112*(3), 441-454.

[8] Asiya, S., & Sugitha, N. (2023). Automatically segmenting and classifying the lung nodules from CT images. *Int J Intell Syst Appl Eng*, *12*(1s), 271-281.

[9] Bhattacharjee, A., Murugan, R., & Goel, T. (2022). A hybrid approach for lung cancer diagnosis using optimized random forest classification and K-means visualization algorithm. *Health and Technology*, *12*(4), 787-800. https://doi.org/10.1007/s12553-022-00679-2.

[10] Bhuvaneswari, C., Aruna, P., & Loganathan, D. (2014). A new fusion model for classification of the lung diseases using genetic algorithm. *Egyptian Informatics Journal*, *15*(2), 69-77.

[11] Biradar, V. G., & Pareek, P. K. (2022,). Lung cancer detection and classification using 2D convolutional neural network. In *2022 IEEE 2nd Mysore Sub Section International Conference (MysuruCon)* 1-5. IEEE. https://doi.org/10.1109/MysuruCon55714.2022.9972595.

[12] Boban, B. M., & Megalingam, R. K. (2020). Lung diseases classification based on machine learning algorithms and performance evaluation. In *2020 international conference on communication and signal processing (ICCSP)*. 0315-0320. IEEE. https://doi.org/10.1109/ICCSP48568.2020.9182324.

[13] Bodduluri, S., Newell Jr, J. D., Hoffman, E. A., & Reinhardt, J. M. (2013). Registration-based lung mechanical analysis of chronic obstructive pulmonary disease (COPD) using a supervised machine learning framework. *Academic radiology*, *20*(5), 527-536. https://doi.org/10.1016/j.acra.2013.01.019.

[14] Chamberlain, D., Kodgule, R., Ganelin, D., Miglani, V., & Fletcher, R. R. (2016). Application of semi-supervised deep learning to lung sound analysis. In *2016 38th Annual international conference of the IEEE engineering in medicine and biology society (EMBC)* (804-807). IEEE. https://doi.org/10.1109/EMBC.2016.7590823

[15] Dai, Q., Ishfaque, M., Khan, S. U. R., Luo, Y. L., Lei, Y., Zhang, B., & Zhou, W. (2024). Image classification for sub-surface crack identification in concrete dam based on borehole CCTV images using deep dense hybrid model. *Stochastic Environmental Research and Risk Assessment*, 1-18. https://doi.org/10.1007/s00477-024-02743-x.

[16] Dhurgadevi, Nandhini, Pavithra, & Suganya. (2022). Pothole Detection Using Deep Learning. *International Academic Journal of Innovative Research, 9*(2), 01–04. https://doi.org/10.9756/IAJIR/V9I2/IAJIR0908.

[17] Emanet, N., Öz, H. R., Bayram, N., & Delen, D. (2014). A comparative analysis of machine learning methods for classification type decision problems in healthcare. *Decision Analytics*, *1*, 1-20. https://doi.org/10.1186/2193-8636-1-6.

[18] Hekmat, A., Zhang, Z., Khan, S. U. R., Shad, I., & Bilal, O. (2025). An attention-fused architecture for brain tumor diagnosis. *Biomedical Signal Processing and Control*, 101, 107221. https://doi.org/10.1016/j.bspc.2024.107221.

[19] Hosseinzadeh, F., KayvanJoo, A. H., Ebrahimi, M., & Goliaei, B. (2013). Prediction of lung tumor types based on protein attributes by machine learning algorithms. *SpringerPlus*, *2*, 1-14.

[20] https://www.kaggle.com/datasets/zhangweiled/lidcidri

[21] Jian, M., Zhang, L., Jin, H., & Li, X. (2023). 3dagnet: 3d deep attention and global search network for pulmonary nodule detection. *Electronics*, *12*(10), 2333. https://doi.org/10.3390/electronics12102333.

[22] Jyothi, B., & Mary Gladence, L. (2024). Enhanced Accuracy for Lung Adenocarcinoma (LUAD) Prediction based UMAP Feature Using Artificial Neural Network. *Journal of Wireless Mobile Networks, Ubiquitous Computing, and Dependable Applications, 15*(4), 380-394. https://doi.org/10.58346/JOWUA.2024.I4.026

[23] Kaplan, A., Cao, H., FitzGerald, J. M., Iannotti, N., Yang, E., Kocks, J. W., ... & Mastoridis, P. (2021). Artificial intelligence/machine learning in respiratory medicine and potential role in asthma and COPD diagnosis. *The Journal of Allergy and Clinical Immunology: In Practice*, *9*(6), 2255-2261. https://doi.org/10.1016/j.jaip.2021.02.014.

[24] Kavitha, M. (2024). Energy-efficient algorithms for machine learning on embedded systems. *Journal of Integrated VLSI, Embedded and Computing Technologies, 1*(1), 16-20. https://doi.org/10.31838/JIVCT/01.01.04

[25] Kazeminia, S., Baur, C., Kuijper, A., Van Ginneken, B., Navab, N., Albarqouni, S., & Mukhopadhyay, A. (2020). GANs for medical image analysis. *Artificial intelligence in medicine*, *109*, 101938. https://doi.org/10.1016/j.artmed.2020.101938.

[26] Kim, G. B., Jung, K. H., Lee, Y., Kim, H. J., Kim, N., Jun, S., ... & Lynch, D. A. (2018). Comparison of shallow and deep learning methods on classifying the regional pattern of diffuse lung disease. *Journal of digital imaging*, *31*, 415-424. https://doi.org/10.1007/s10278-017-0028-9.

[27] Koth, L. L., Solberg, O. D., Peng, J. C., Bhakta, N. R., Nguyen, C. P., & Woodruff, P. G. (2011). Sarcoidosis blood transcriptome reflects lung inflammation and overlaps with tuberculosis. *American journal of respiratory and critical care medicine*, *184*(10), 1153-1163. https://doi.org/10.1164/rccm.201106-1143OC

[28] Kovalev, V., & Kazlouski, S. (2019). Examining the capability of GANs to replace real biomedical images in classification models training. In *Pattern Recognition and Information Processing: 14th International Conference, PRIP 2019, Minsk, Belarus, May 21–23, 2019, Revised Selected Papers 14* (pp. 98-107). Springer International Publishing. https://doi.org/10.1007/978-3-030-35430-5_9

[29] Lin, J., She, Q., & Chen, Y. (2023). Pulmonary nodule detection based on IR-UNet++. *Medical & Biological Engineering & Computing*, *61*(2), 485-495. https://doi.org/10.1007/s11517-022-02727-5.

[30] Ma, Y., Xu, X., Yu, Q., Zhang, Y., Li, Y., Zhao, J., & Wang, G. (2019). Lungbrn: A smart digital stethoscope for detecting respiratory disease using bi-resnet deep learning algorithm. In *2019 IEEE Biomedical Circuits and Systems Conference (BioCAS)* (pp. 1-4). IEEE. https://doi.org/10.1109/BIOCAS.2019.8919021

[31] Mkindu, H., Wu, L., & Zhao, Y. (2023). Lung nodule detection of CT images based on combining 3D-CNN and squeeze-and-excitation networks. *Multimedia Tools and Applications*, *82*(17), 25747-25760.

[32] Nguyen, T. C., Nguyen, T. P., Cao, T., Dao, T. T. P., Ho, T. N., Nguyen, T. V., & Tran, M. T. (2023). MANet: Multi-branch attention auxiliary learning for lung nodule detection and segmentation. *Computer Methods and Programs in Biomedicine*, *241*, 107748. https://doi.org/10.1016/j.cmpb.2023.107748.

[33] O'Neil, A., Shepherd, M., Beveridge, E., & Goatman, K. (2017). A comparison of texture features versus deep learning for image classification in interstitial lung disease. In *Medical Image Understanding and Analysis: 21st Annual Conference, MIUA 2017, Edinburgh, UK, July 11–13, 2017, Proceedings 21* (743-753). Springer International Publishing.

[34] Palaniappan, R., Sundaraj, K., & Sundaraj, S. (2014). A comparative study of the svm and k-nn machine learning algorithms for the diagnosis of respiratory pathologies using pulmonary acoustic signals. *BMC bioinformatics*, *15*, 1-8. https://doi.org/10.1186/1471-2105-15-223.

[35] Paraschiv, E. A., & Rotaru, C. M. (2020). Machine learning approaches based on wearable devices for respiratory diseases diagnosis. In *2020 International Conference on e-Health and Bioengineering (EHB)*. 1-4. IEEE. https://doi.org/10.1109/EHB50910.2020.9280098.

[36] Poreva, A., Karplyuk, Y., & Vaityshyn, V. (2017). Machine learning techniques application for lung diseases diagnosis. In *2017 5th IEEE Workshop on Advances in Information, Electronic and Electrical Engineering (AIEEE)* (pp. 1-5). https://doi.org/10.1109/AIEEE.2017.8270528

[37] Prasad, B. D. C. N., PESN Krishna Prasad, and Yeruva Sagar. "A comparative study of machine learning algorithms as expert systems in medical diagnosis (Asthma)." *In Advances in Computer Science and Information Technology: First International Conference on Computer Science and Information Technology, CCSIT 2011, Bangalore, India, January 2-4, 2011. Proceedings, Part I 1*, pp. 570-576. Springer Berlin Heidelberg, 2011.

[38] Puri, A., & Lakhwani, K. (2013). Enhanced approach for handwritten text recognition using neural network. *International Journal of Communication and Computer Technologies*, *1*(2), 79-82. https://doi.org/10.31838/IJCCTS/01.02.02

[39] Radhika, P. R., Nair, R. A., & Veena, G. (2019). A comparative study of lung cancer detection using machine learning algorithms. In *2019 IEEE international conference on electrical, computer and communication technologies (ICECCT)*. 1-4. IEEE. https://doi.org/10.1109/ICECCT.2019.8869001.

[40] Rehman, A., Kashif, M., Abunadi, I., & Ayesha, N. (2021, April). Lung cancer detection and classification from chest CT scans using machine learning techniques. In *2021 1st international conference on artificial intelligence and data analytics (CAIDA)*. 101-104. IEEE. https://doi.org/10.1109/CAIDA51941.2021.9425269.

[41] Saikia, T., Kumar, R., Kumar, D., & Singh, K. K. (2022). An automatic lung nodule classification system based on hybrid transfer learning approach. *SN Computer Science*, *3*(4), 272. https://doi.org/10.1007/s42979-022-01167-0.

[42] Sarwar, A., & Sharma, V. (2014). Comparative analysis of machine learning techniques in prognosis of type II diabetes. *AI & society*, *29*, 123-129. https://doi.org/10.1007/s00146-013-0456-0.

[43] Sathish Kumar, T. M. (2024). Developing FPGA-based accelerators for deep learning in reconfigurable computing systems. *SCCTS Transactions on Reconfigurable Computing, 1*(1), 1-5. https://doi.org/10.31838/RCC/01.01.01

[44] Sathish, R., & Ravichandran, K. S. (2018). Integrated Optimization of Network Topology and DG Output for MVDC Distribution Systems. *International Journal of Advances in Engineering and Emerging Technology*, *9*(3), 91–103. https://erlibrary.org/erl/index.php/ijaeet/article/view/237

[45] Shahzad, I., Khan, S. U. R., Waseem, A., Abideen, Z. U., & Liu, J. (2024). Enhancing ASD classification through hybrid attention-based learning of facial features. *Signal, Image and Video Processing*, *18*(Suppl 1), 475-488. https://doi.org/10.1007/s11760-024-03167-4

[46] Sharifi, H., Lai, Y. K., Guo, H., Hoppenfeld, M., Guenther, Z. D., Johnston, L., ... & Hsu, J. L. (2020). Machine learning algorithms to differentiate among pulmonary complications after hematopoietic cell transplant. *Chest*, *158*(3), 1090-1103. https://doi.org/10.1016/j.chest.2020.02.076

[47] Trusculescu, A. A., Manolescu, D., Tudorache, E., & Oancea, C. (2020). Deep learning in interstitial lung disease—how long until daily practice. *European radiology*, *30*(11), 6285-6292. https://doi.org/10.1007/s00330-020-06986-4.

[48] Wang, C., Chen, X., Du, L., Zhan, Q., Yang, T., & Fang, Z. (2020). Comparison of machine learning algorithms for the identification of acute exacerbations in chronic obstructive pulmonary disease. *Computer methods and programs in biomedicine*, *188*, 105267. https://doi.org/10.1016/j.cmpb.2019.105267

Authors Biography

Asiya obtained her Bachelor's degree in Computer Science & Engineering from BITS, Warangal, Telangana State India. Then she obtained her Master's degree in Computer Networks and Information Systems and pursuing PhD in Computer Science & Engineering major in Artificial Intelligence with image processing from Noorul Islam Centre for Higher Education, Tamil Nadu, India. Currently, she is working as a Assistant Professor in School of Computer Science and Artificial Intelligence at SR University Warangal, India. Her specializations include Artificial Intelligence, Internet of Things, Machine Learning, Image Processing, Neural Networks, Cloud Computing, Network Security. Her current research interests are Artificial Intelligence, Image Processing, Machine Learning

Dr.N. Sugitha received B. E degree in Electronics and Communication Engineering from Manonmaniam Sundaranar University, Tamil Nadu, India in the year 1997.She received her M.E degree in Communication Systems from Madurai Kamaraj University, Tamil Nadu. India. In the year 2000. She has been awarded with Ph.D degree for her work "Image Denoising using Combined Spatial and Multiresolution Filters" by Anna University, Chennai, Tamil Nadu, India in 2015.Presently she is working as Associate Professor in the Department of Electronics and Communication Engineering. She has 22 years of teaching and research experience. She has published/presented more than 40 technical papers in International/National journals and conferences. Sheisa life Member in Indian Society for Technical Education (ISTE).